Optics Communications 284 (2011) 15–19

Contents lists available at ScienceDirect

Optics Communications

journal homepage: www.elsevier.com/locate/optcom

Dual-axes differential confocal microscopy with high axial resolution and long working distance

Weiqian Zhao *, Qin Jiang, Lirong Qiu, Dali Liu

Key Laboratory of Photoelectronic Imaging Technology and System (Ministry of Education of China), Opto-Electronic College, Beijing Institute of Technology, Beijing 100081, PR China

ARTICLE INFO

Article history:
Received 29 June 2010
Received in revised form 11 August 2010
Accepted 16 August 2010

Keywords:
Confocal microscopy
Dual-axes differential confocal microscopy (DDCM)
Thickness measurement
Tracing measurement

ABSTRACT

We discover that the slight transverse offset of a point detector results in a shift of the axial intensity response curve in a dual-axes confocal microscopy (DCM). Based on this, we propose a new dual-axes differential confocal microscopy (DDCM) with high axial resolution and long working distance, in which two point detectors are placed symmetrically about the collection axis. And a signal is obtained through the differential subtraction of two signals received simultaneously by the two point detectors. Theoretical analyses and preliminary experiments indicate that DDCM is feasible and suitable for the high precision tracing measurement of microstructures and surface contours.

1. Introduction

For its high resolution and unique optical sectioning capability, confocal microscopy is widely used in microelectronics, material, industrial precision measurement and biomedicine. Udupa et al., for example, proposed a confocal scanning optical microscope for the measurement of two-dimensional (2-D) surface roughness, 3-D surface topography and form errors [1,2]. Whereas the confocal microscopy used for the measurement of microstructures and surface contours has no absolute zero, and is inconvenient for the precise tracing measurement. In order to achieve the bipolar absolute tracing measurement, we developed a superresolution differential confocal microscopy with a dual-receiving light path, by using the differential subtraction of two signals from two detectors with an axial offset [3,4]. However, the use of two detectors makes the structure complicated and the adjustment stringent. And the difference between two detectors could bring measurement error.

The aforementioned confocal microscopy needs a high numerical aperture (NA) objective to achieve a high resolution, but this will reduce the working distance (WD) and cause the difficulty in the practical measurement. In order to improve the resolution and WD simultaneously, T. Wang et al. proposed a dual-axes confocal microscopy (DCM) [5–7], which observes the sample at an angle to the illumination axis.

Based on DCM, we discover that the slight transverse offset of a point detector results in a shift of its axial intensity response curve. So we propose a new dual-axes differential confocal microscopy (DDCM) with high axial resolution, long WD. Moreover, DDCM has an absolute zero that is convenient for the measurement range extension and high precision tracing measurement for microstructures and surface contours.

The rest of the paper is organized as follow. Section 2 describes the effect of point detector transverse offset in DCM and the principle of DDCM. Following this, the calculation of the optimum point detector offset is also detailed in Section 2. To evaluate the feasibility of DDCM, Section 3 provides verification measurement of DDCM axial response, and also provides the measurement of a cover-glass thickness to verify the DDCM superiority for the tracing measurement. Section 4 contains the conclusion of this study.

2. DDCM principle

2.1. Principle

As shown in Fig. 1, the illumination lens (IL) and the collection lens (CL) have the same parameters, illumination axis IA and collection axis CA cross axis z at angle θ. (x_d,y_d,z_d) is the coordinate of the lens CL in the detection space, and (x,y,z), (x_i,y_i,z_i) and (x_c,y_c,z_c) are the coordinates of DDCM, lens IL and lens CL in the sample space, respectively, and

$$\begin{cases} x_i = x\cos\theta - z\sin\theta \\ y_i = y \\ z_i = x\sin\theta + z\cos\theta \end{cases} \tag{1}$$

* Corresponding author.
E-mail address: zwq669@126.com (W. Zhao).

0030-4018/$ – see front matter © 2010 Elsevier B.V. All rights reserved.
doi:10.1016/j.optcom.2010.08.033

$$\begin{cases} x_c = x\cos\theta + z\sin\theta \\ y_c = y \\ z_c = -x\sin\theta + z\cos\theta \end{cases} \tag{2}$$

When we use an objective of NA<0.7 in DDCM, the scalar paraxial theory can be applied to the theoretical deduction. If the point detector has transverse offset M in the x_d direction, the illumination point spread function (PSF) $h_i(x_i,y_i,z_i)$ and collection PSF $h_c(x_c,y_c,z_c,v_M)$ are [8]

$$h_i(x_i,y_i,z_i) = \int\int_{-\infty}^{+\infty} P\left(x_\rho,y_\rho\right)\exp\left[\frac{iu_i}{2}\left(x_\rho^2+y_\rho^2\right)\right] \times\exp\left[i\left(v_{ix}x_\rho+v_{iy}y_\rho\right)\right]dx_\rho dy_\rho, \tag{3}$$

$$h_c(x_c,y_c,z_c,v_M) = \int\int_{-\infty}^{+\infty} P\left(x_\rho,y_\rho\right)\exp\left[\frac{iu_c}{2}\left(x_\rho^2+y_\rho^2\right)\right] \times\exp\left\{i\left[(v_{cx}+v_M)x_\rho+v_{cy}y_\rho\right]\right\}dx_\rho dy_\rho. \tag{4}$$

where $v_{ix}=2\pi x_i\sin\alpha/\lambda$, $v_{iy}=2\pi y_i\sin\alpha/\lambda$ and $u_i=8\pi z_i\sin^2(\alpha/2)/\lambda$ are the lens IL optical normalized coordinates, $v_{cx}=2\pi x_c\sin\alpha/\lambda$, $v_{cy}=2\pi y_c\sin\alpha/\lambda$ and $u_c=8\pi z_c\sin^2(\alpha/2)/\lambda$ are the lens CL optical normalized coordinates, and $v_M=2\pi M\sin\alpha_d/\lambda$ is the optical normalized coordinate corresponding to M. λ is the laser wavelength, α is the lenses IL and CL semi-angular aperture in the sample space, and α_d is the lens CL semi-angular aperture in the detection space. $P(x_\rho,y_\rho)$ is the lenses IL and CL pupil function, coordinates x_ρ and y_ρ are the distance in the pupil plane of lenses IL and CL normalized by the pupil radius.

Supposing $x=y=0$, we can obtain the axial intensity response $I(z,v_M)$ with point detector offset from Eqs. (3) and (4), and

$$I(z,v_M) = |h_i(x_i,y_i,z_i)\times h_c(x_c,y_c,z_c,v_M)|^2. \tag{5}$$

With $\lambda=632.8$ nm, $\theta=45°$ and NA$=0.13$, when v_M are ±2.0, ±1.3, and 0.0, respectively, the normalized axial intensity response curves $I(z,v_M)$ are shown in Fig. 2. It can be seen from Fig. 2 that curves $I(z,v_M)$ have shifts from curve $I(z,\ v_M=0.0)$ only in the z direction. That is, the offset of the point detector in the x_d direction results a shift of the DCM axial intensity response.

Based on this property, we use two point detectors to receive signals $I_A(z,-v_M)$ and $I_B(z,+v_M)$ simultaneously, then we can obtain

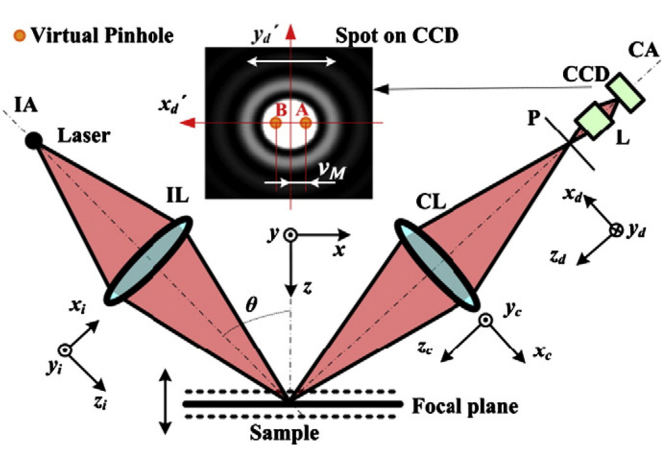

Fig. 1. DDCM principle.

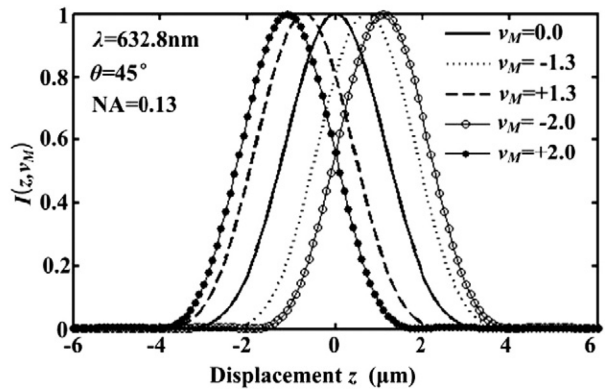

Fig. 2. Axial response curves with different v_M.

DDCM axial intensity response curve $I_D(z,v_M)$ through the differential subtraction of the two signals, and

$$\begin{aligned} I_D(z,v_M) &= I_A(z,-v_M)-I_B(z,+v_M) \\ &= |h_i(x_i,y_i,z_i)\times h_c(x_c,y_c,z_c,-v_M)|^2 \\ &\quad -|h_i(x_i,y_i,z_i)\times h_c(x_c,y_c,z_c,+v_M)|^2 \end{aligned} \tag{6}$$

Fig. 3 shows the DDCM normalized axial intensity response curve $I_D(z,v_M=1.3)$ and DCM normalized axial intensity response curve $I(z,\ v_M=0)$ under the same conditions. It can be seen from Fig. 3 that DDCM has the following advantages. 1) It has absolute zero O in linear interval cd with the maximum sensitivity, which corresponds to the objective focus and can be used for the bipolar tracing measurement. 2) It has a high axial resolution because the slope in linear interval cd of curve $I(z,v_M=1.3)$ is about twice higher than that in linear interval ab of curve $I(z,v_M=0)$. 3) It works in linear interval cd, so it has a good linearity and a wide linear measurement range.

The key to DDCM is how to detect signals $I_A(z,-v_M)$ and $I_B(z,+v_M)$. Therefore, we use objective L to magnify the spot in focal plane P and image it on a CCD. As shown in Fig. 4, when the sample is in the DDCM focal plane, we set the spot centre as the origin to establish reference coordinate (x_d',y_d') in the CCD image plane. We symmetrically place two circular virtual pinholes A and B with offset v_M on axis x_d', and use the CCD to receive signals $I_A(z,-v_M)$ and $I_B(z,+v_M)$ within regions A and B, then obtain DDCM axial response curve $I_D(z,v_M)$ through the differential subtraction of $I_A(z,-v_M)$ and $I_B(z,+v_M)$. This method uses one CCD to achieve the dual-receiving light path arrangement, which can simplify the structure and avoid the error caused by the difference between two detectors.

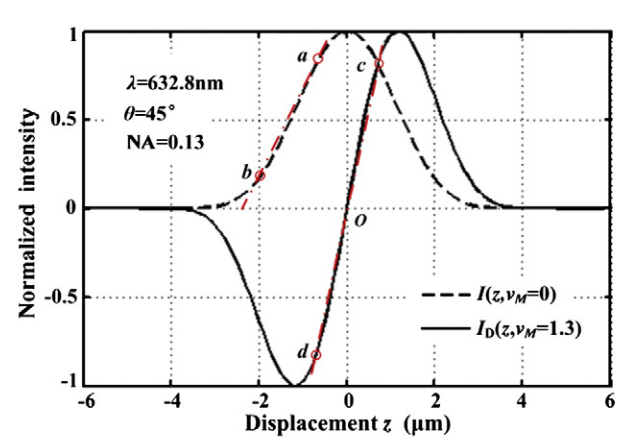

Fig. 3. Theoretical axial response curves.

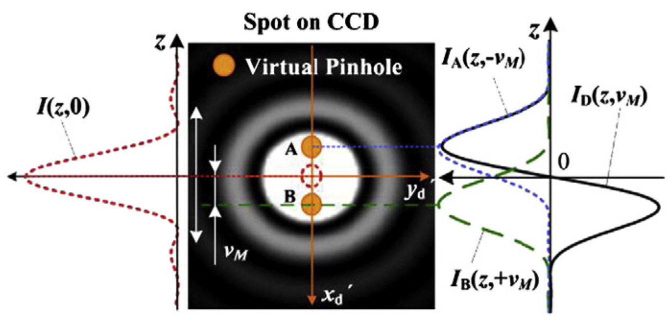

Fig. 4. DDCM detection principle.

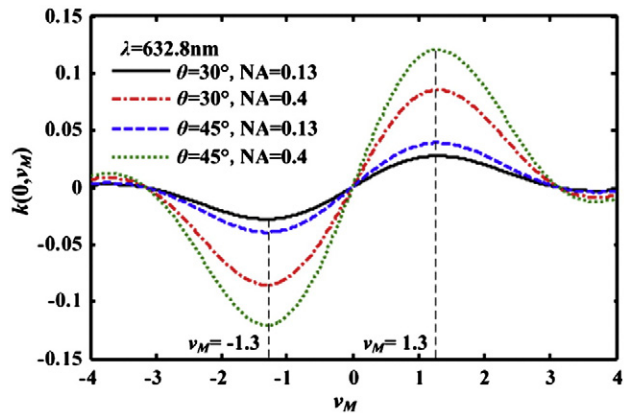

Fig. 6. Variation of gradient curve $k(0,v_M)$ with v_M.

2.2. Optimum v_M

It can be seen from Fig. 5 obtained by use of Eq. (6) that v_M has an optimum value that can be used to optimize the resolution property of axial response curve. Gradient $k(z,v_M)$ obtained by use of differentiation of the differential signal $I_D(z,v_M)$ on z is

$$k(z, v_M) = \frac{\partial I_D(z, v_M)}{\partial z}, \tag{7}$$

where $k(0,v_M)$ and $k(z,v_M)$ are equal in the linear range, and the gradient in the linear measurement range of $I_D(z,v_M)$ at $z=0$ can be expressed in $k(0, v_M)$ as shown in Eq. (8). And

$$k(0, v_M) = C\frac{\mathrm{NA}\sin\theta\sin v_M}{\lambda v_M^3}(\sin v_M - v_M\cos v_M), \tag{8}$$

where C is a constant. It should be noted that λ, θ and NA have no effect on the location of v_M corresponding to the $k(0,v_M)$ extreme. Fig. 6 shows $k(0,v_M)$ curves and the optimum v_M can be obtained when the absolute values of $k(0,v_M)$ are largest at $v_M = \pm 1.3$.

3. Experiment

3.1. Axial response experiment

To verify the DDCM feasibility, we build an experimental setup based on Fig. 1. As shown in Fig. 7, the light source used is a semiconductor laser with λ = 632.8 nm, the sample used is a mirror, and CCD used is WATEC 902H2 Ultimate with the effective pixels of 752(H)×582(V) and unit cell size of 8.6 μm (H)×8.3 μm (V). The high-precision air bearing slider is used as the workbench actuator, and XL-80 interferometer produced by RENISHAW is used to measure the displacement of the sample. Lenses IL and CL have NA of 0.13 and focal-length of 31 mm.

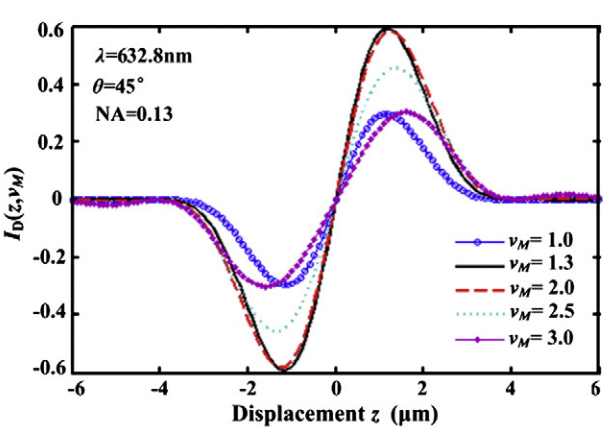

Fig. 5. DDCM axial response curves for different v_M.

Illumination axis z_i is oriented at $\theta = 45°$ to axis z. WD is about 21 mm. The focal-length of lens L_t is 200 mm, and the spot diameter in the L_t focal plane is about 38 μm. The magnification of objective L is 25$^{\times}$, and the spot diameter on the CCD is about 950 μm. And virtual pinholes A and B with a diameter of about 50 μm have a transverse offset of 161.2 μm corresponding to $v_M = 1.3$.

The light from the laser is collimated by an extender lens and becomes a parallel beam with the same diameter as the entrance pupil of lens IL, and focused onto the mirror by lens IL. The light reflected from the mirror is collected by lens CL, focused by lens L_t and then imaged on the CCD by objective L. When the mirror is in the focal plane, we establish reference coordinate (x_d´, y_d´) in the CCD image plane, and place pinholes A and B at points (−161.2 μm, 0) and (+161.2 μm, 0), respectively. When the mirror moves along axis z, we calculate the grey summations of pixels within regions A and B, respectively, to get axial response curves $I_A(z,-v_M)$ and $I_B(z,+v_M)$, then we obtain curve $I_D(z,v_M)$ through the differential subtraction of $I_A(z,-v_M)$ and $I_B(z,+v_M)$. Similarly, we set a new virtual pinhole with the same radius at the origin of the coordinate (x_d´, y_d´) to get an axial response curve $I(z,0)$. Normalized curves $I_D(z,v_M)$ and $I(z,0)$ are shown in Fig. 8.

It can be seen from Fig. 8 that the experimental curves are in good agreement with the theoretical curves shown in Fig. 3. And curve $I(z,0)$ has a measurement range of 1.17 μm and a slope of 0.518 in linear interval ab, while curve $I_D(z,v_M)$ has a measurement range of

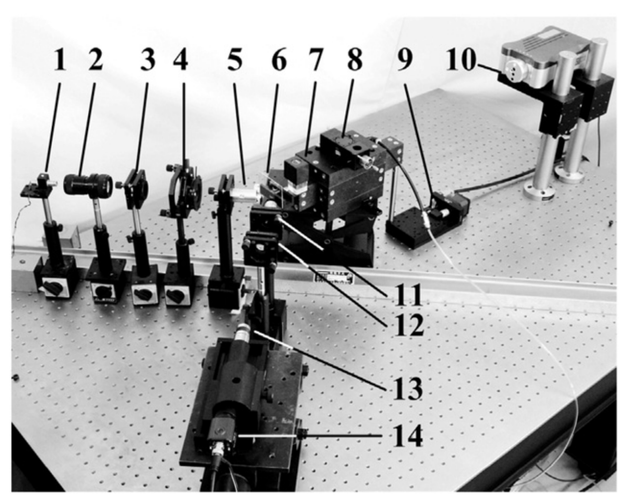

Fig. 7. Experimental setup. 1. Semiconductor laser. 2. Extender lens. 3. Attenuating plate. 4. Aperture stop. 5. IL. 6. Mirror. 7. Air bearing slider. 8. Interferometer measurement prisms. 9. Motorized precision translation stage. 10. XL-80 interferometer produced by RENISHAW. 11. CL. 12. L_t. 13. L. 14. CCD.

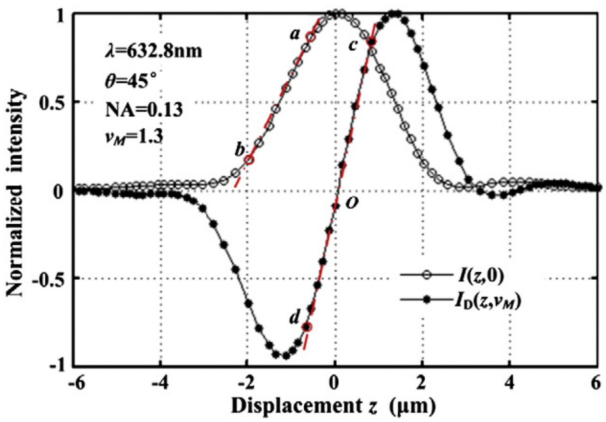

Fig. 8. Experimental axial response curves.

1.33 μm and a slope of 1.128 in linear interval *cd*. Therefore curve $I(z, v_M)$ has a slope of about 2 times higher than curve $I(z,0)$ in the linear interval.

3.2. Thickness measurement of a cover-glass

In order to verify the DDCM superiority for the tracing measurement, we measure the thickness of a cover-glass using the absolute zero of DDCM axial response curve and the peak of DCM axial response curve, respectively. The nominal refractive index of the cover-glass is $n=1.5163$, and the nominal thickness is $d_0=168.00$ μm. When the cover-glass is moved along axis z, DCM and DDCM both obtain the axial response curves near its front and back surfaces and use the peaks and absolute zeroes to precisely identify the positions of the front and back surfaces. Then the thickness can be calculated using the equation as shown in Eq. (9) [9]

$$d = n\Delta z / g \tag{9}$$

where g is a factor relating to refractive index n and incident angles θ. For $n=1.5163$ and $\theta=45°$, the value of g is 0.8 [9].

The measured curves are shown in Figs. 9 and 10. As shown in Fig. 9, the coordinates of peaks P_1 and P_2 of DCM axial response curves $I_{P1}(z)$ and $I_{P2}(z)$ are $z_{P1}=1.81$ μm and $z_{P2}=89.76$ μm, and $\Delta z_P=z_{P2}-z_{P1}=87.95$ μm. As shown in Fig. 10, the coordinates of absolute zeroes O_1 and O_2 of DDCM axial response curves $I_{O1}(z)$ and $I_{O2}(z)$ are $z_{O1}=1.70$ μm and $z_{O2}=89.91$ μm, and $\Delta z_O=z_{O2}-z_{O1}=88.21$ μm.

Then the thicknesses measured by DCM and DDCM are $d_P=166.70$ μm and $d_O=167.19$ μm, respectively. And the relative measurement errors are $\Delta\delta_P=(d_0-d_P)/d_0\times 100\%=0.8\%$ and $\Delta\delta_O=(d_0-d_O)/d_0\times 100\%=0.5\%$, respectively. The experimental results indicate that the measurement accuracy by the absolute zero of DDCM is superior to that by the peak of DCM for the tracing measurement.

4. Conclusion

We proposed a new dual-axes differential confocal microscopy, which uses one CCD to achieve the dual-receiving light path arrangement. This new approach has high axial resolution, long WD and absolute zero but also a simple structure, and can provide a new technique for the measurement of microstructures and surface contours.

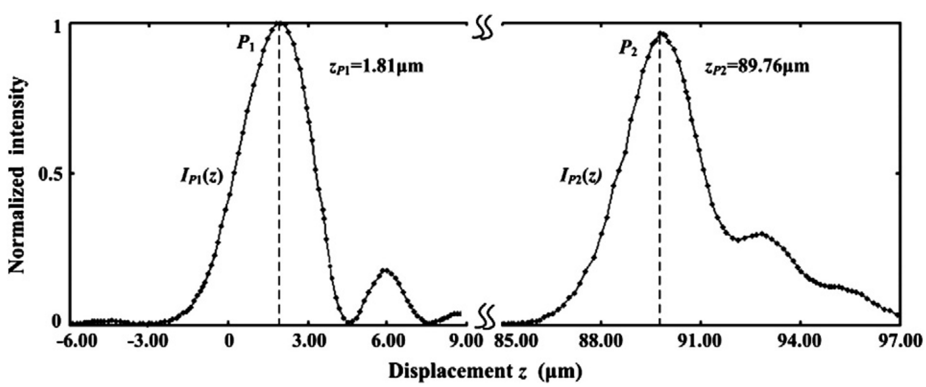

Fig. 9. Measurement curves by DCM.

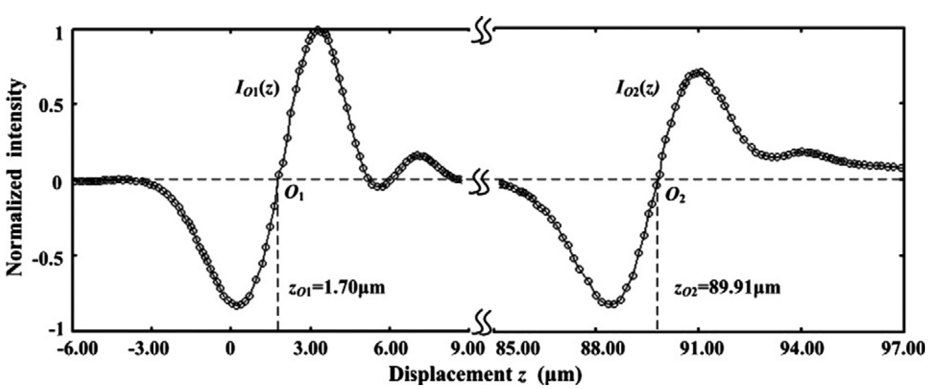

Fig. 10. Measurement curves by DDCM.

Acknowledgment

Thanks to the National Science Foundation of China (Nos. 60708015 and 60927012), Excellent and Young Scholars Research Fund of Beijing Institute of Technology, and Research Foundation for the Doctoral Program of Higher Education of China (No. 20091101110018) for the support.

References

[1] G. Udupa, M. Singaperumal, R. Sirohi, et al., Meas. Sci. Technol. 11 (2000) 305.
[2] G. Udupa, M. Singaperumal, R. Sirohi, et al., Meas. Sci. Technol. 11 (2000) 315.
[3] W. Zhao, J. Tan, L. Qiu, Opt. Express 12 (2004) 5013.
[4] W. Zhao, J. Tan, L. Qiu, et al., Meas. Sci. Technol. 16 (2005) 497.
[5] T. Wang, M. Mandella, C.H. Contag, et al., Opt. Lett. 28 (2003) 414.
[6] T. Wang, C. Contag, M. Mandella, et al., J. Biomed. Opt. 9 (2004) 735.
[7] G. Kino, T. Wang, C. Contag, et al., Proc. SPIE 5324 (2004) 35.
[8] M. Gu, Principles of Three-Dimensional Imaging in Confocal Microscopes, World Scientific Publishing, Singapore, 1996, Chap.3.
[9] L. Li, Y. Huang, Y. Wang, Applied Optics, Beijing Institute of Technology Press, Beijing, 2005, p. 100.